

A Robust Power Control Strategy to Enhance LVRT Capability of Grid-Connected DFIG-Based Wind Energy Systems

Sid Ahmed El Mehdi Ardjoun^{1*}, Mouloud Denai² and Mohamed Abid¹

¹IRECOM Laboratory, Faculty of Electrical Engineering, Djillali Liabes University, Sidi Bel-Abbes, Algeria.

²School of Engineering and Technology, University of Hertfordshire, Hatfield, United Kingdom.

Corresponding Author: elmehdi.ardjoun@univ-sba.dz

Abstract

This paper presents a new robust and effective control strategy to mitigate symmetrical voltage dips in a grid-connected doubly-fed induction generator (DFIG) wind energy conversion system without any additional hardware in the system. The aim is to control the power transmitted to the grid so as to keep the electrical and mechanical quantities above their threshold protection values during a voltage dip transient. To achieve this, the references of the powers are readjusted to adapt the wind energy conversion system to the fault conditions. Robust control strategies, combining the merits of sliding mode theory and fuzzy logic are then proposed in this paper. These controllers are derived from the dynamic model of the DFIG considering the variations in the stator flux generated by the voltage drop. This approach is found to yield better performance than other control design methods which assume the flux in the stator to remain constant in amplitude. This control scheme is compliant with the fault-ride-through grid codes which require the wind turbine generator to remain connected during voltage dips. A series of simulations scenarios are carried out on a 3 MW wind turbine system to demonstrate the effectiveness of the proposed control schemes under voltage dips and parameters uncertainties conditions.

Keywords

Wind turbine, doubly-fed induction generator, powers control, fuzzy sliding mode control, voltage dip.

Nomenclature	
V_w	wind speed (m/s)
R	rotor radius (m)
Ω	DFIG rotor speed (rpm)
J	turbine total inertia ($\text{kg}\cdot\text{m}^2$)
f	turbine total friction coefficient ($\text{Nm}\cdot\text{s}/\text{rad}$)
v, i	voltage (V), current (A)

Control of Wind Energy Systems to Improve LVRT

P, Q	real power (W), reactive power (VAR)
T_{em}	electromagnetic torque (Nm)
R_r, R_s	rotor and stator resistance (Ω)
L_r, L_s	rotor and stator inductance (H)
φ	flux (Wb)
M	mutual inductance (H)
σ	leakage coefficient $\sigma = 1 - M^2 / L_s L_r$
θ_r, θ_s	rotor and stator position angle (rad)
ω_r, ω_s	angular speed, synchronous speed (rad/s)
N_p	number of pole pairs
X^d	desired signal
X	state variable of the control signal
λ	positive coefficient
n	system order

Acronyms	
DFIG	doubly fed induction generator
LVRT	low-voltage ride-through
RSC	rotor side converter
GSC	grid side converter
VC	vector control
FSMC	fuzzy sliding mode control
MPPT	maximum power point tracking

1. Introduction

Electric power quality has become a vitally important issue that involves all actors, whether they are network managers or users of these networks. The term ‘power quality’ is a broad concept which covers both the continuity of the electrical supply and the quality of the voltage and current waveforms. The main phenomena that can affect this quality are frequency and voltage fluctuations, voltage dips, harmonic currents or voltages.

The continuity of electricity supply may be affected by a fault in the network (e.g. voltage dip) which may result in the disconnection of a generation unit. This causes a deficit in the supply of power to the loads and a loss of the electrical network stability.

A voltage dip is a sudden drop in the voltage which ranges between 10% and 90% of its nominal value, and which may last from ten milliseconds up to one minute.¹ A voltage dip can be due to several reasons: a short circuit in the network, a partial disconnection of the power supply, heavy currents due to the starting of large motors, and large currents due to electric arcs or saturation of transformers.²

Control of Wind Energy Systems to Improve LVRT

With the increasing penetration of wind energy in distribution grids, many countries around the world have started to impose new grid codes which establish the guidelines and requirements for the interconnection of wind generators to the grid.³ One of the most stringent technical requirements for the grid-connection of wind generators is their ability to resist to voltage disturbances in the network. To fulfill this technical requirement, generators should remain connected to the network and should be able to regain normal operation after the occurrence of a fault. This capability of the generator to stay connected is defined by the term low-voltage ride through (LVRT).

Currently, the DFIG is the most commonly used variable-speed generator in wind power applications. However, it is very sensitive to network disturbances and more particularly to voltage dips.⁴

Voltage drops, even located far from the DFIG, can cause an over-intensity of current in both the rotor and stator of the machine, and an overvoltage at the DC bus. Without protections, this may lead to the deterioration of the power converters and possibly their breakdown.⁵ Moreover, these voltage drops are accompanied by an over-speed of the turbine which deteriorates its normal operation.⁶

Several researchers have addressed the concept of LVRT during network faults and proposed control strategies for the DFIG which can be divided into two classes: A real method based on improving the control strategy of the DFIG and a passive method which consists of introducing hardware protections.⁷ Table 1 gives a summary of these methods.

TABLE 1 LVRT methods for a wind system

Real methods	Passive methods
Blade pitch angle control	Energystorage
	Crowbar
Control improvement (RSC, GSC)	FACTS devices (SVC, STATCOM, DVR)
	Capacitysizing

In,⁸ the authors propose the use of energy storage systems connected to the DC bus via a DC-DC converter. When the fault occurs, these devices absorb the excess of energy at the DC link, and thus protect the converters against over-voltages. After clearance of the fault, this energy is re-injected into the grid. These energy storage devices are essentially batteries,⁹ or super-capacitors.¹⁰

Crowbar systems are mainly employed to dissipate real power during network faults.¹¹ A crowbar circuit consists of a high-power resistor in series with a switch. The advantages of

Control of Wind Energy Systems to Improve LVRT

this structure are its low cost and simplicity of its control structure. However, crowbar systems cannot improve the injection of reactive power to the grid.

FACTS (Flexible AC Transmission Systems) are another option for keeping wind systems connected to the grid in case of a fault. Examples of these are the STATCOM (Static Compensator) and the SVC (Static Var Compensator). In general, they are used to increase the reactive power control capacity.¹² Another device is the DVR (Dynamic Voltage Restorer) which works by injecting a compensating voltage through a transformer to support the grid during a voltage dip.¹³ All these methods are based on the addition of hardware devices which increase the total cost of the system. Alternatively, other works have focused on modifying converter control strategies.

For the real LVRT methods, different control approaches have been proposed. In,¹⁴ the authors studied the performance limits of vector control. Direct torque control, direct power control, adaptive control and predictive control were also investigated.¹⁵⁻¹⁸

Most variable-speed wind turbine systems use vector control, which can be modified to meet the LVRT requirements of grid operators. The authors in¹⁹ proposed a modified vector control scheme by introducing the variation of flux in the coupling terms between the d-and q-axes. This control approach was further extended to include both the flux magnitude and phase angle,²⁰ and in,²¹ an improved version of this control scheme was proposed.

Other more advanced control strategies have also been proposed to overcome the limitations of classical proportional and integral (PI) controllers. Among these, sliding mode control,²² second-order sliding mode control,²³ fuzzy type-2 control,²⁴ fuzzy control tuning by genetic algorithms,²⁵ fuzzy second order integral terminal sliding mode control,²⁶ passivity control,²⁷ and backstepping control.²⁸

To sum up, whichever the method used, for the wind turbine to fulfill the LVRT requirements, three physical quantities must be closely controlled during a voltage dip to prevent their protections to trigger. These quantities are: the rotational speed of the generator, the stator and rotor currents, and the DC bus voltage. The LVRT capability requires that the wind turbine system must be able to limit, store and/or dissipate real power and contribute to restore the voltage by injecting reactive power.

The authors in,²⁹ presented a comprehensive review of the existing methods and future trends of the DFIG in compliance with LVRT requirements. They concluded that if RSC can counter the grid disturbance effect then the use of additional hardware such as crowbar, DC chopper, etc. can be avoided. They finally suggested to focus more on the development of robust nonlinear control techniques.

Control of Wind Energy Systems to Improve LVRT

In all these previous works, the authors assumed that the flux in the stator is constant in amplitude to simplify the design of their controllers. However, during a voltage dip, since the stator is directly connected to the network, the stator flux is expected to decrease. Therefore, neglecting the dynamics of the stator flux may deteriorate the transient performance of the system during fault conditions.

The solution proposed in this article is to re-adjust the references of the powers so that during the fault the real power is reduced, and the reactive power is injected to help the voltage return to its nominal value. The control scheme proposed to regulate the powers to their reference values is based on Fuzzy Sliding Mode Control (FSMC) concept. The design of the controller is carried out considering the dynamics of the stator flux generated by the voltage dip. The aim is to control the real and reactive powers of a DFIG-based wind turbine system to keep the electrical and mechanical quantities above their threshold values during a voltage dip.

This paper is organized as follows: Section 2 describes the problems of the grid-connected DFIG wind energy conversion system during voltage dip, and presents the solution to the LVRT requirement. Section 3 is devoted to the modeling of the system in view of the RSC control. The proposed FSMC control scheme is derived in Section 4. Finally, the simulation results and conclusion are presented in Section 5 and 6 respectively.

2. Problem Statement and Proposed Solution

The wind energy conversion system (WECS) studied in this paper is based on a DFIG and is depicted in Figure 1. The WECS power electronics interface with the grid consists of two converters: the Rotor Side Converter (RSC) for the control of the real and reactive stator power of the DFIG and the Grid Side Converter (GSC) for the control of the DC bus voltage and reactive power exchanged with the network.

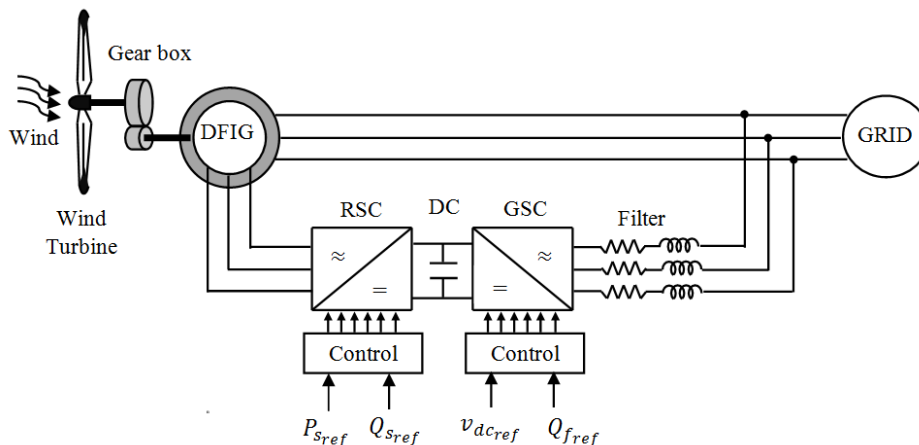


FIGURE 1 Wind energy conversion system based on a DFIG.

Control of Wind Energy Systems to Improve LVRT

Under normal operating conditions, the generated electrical power P_{elec} is equal to the power recovered by the turbine P_t (when losses are neglected). Since the stator of the DFIG is directly coupled to the grid, if a fault such as a voltage dip occurs, the generator magnetic field and rotational speed will be directly affected and consequently this will limit the power transmitted to the grid. At the appearance of the voltage dip, the power captured by the turbine will be greater than the power transmitted to the grid. This causes an over-intensity of current in both the rotor and stator in order to compensate for the decrease in the power caused by the voltage dip.

The problem lies in the management of the excess power $\Delta P = P_t - P_{elec}$ inside the system. To ensure that the LVRT is fulfilled, this excess of power must not cause any electrical and mechanical quantities of the DFIG to drift above their threshold values and trigger the protection.

To protect the system during voltage dips, grid operators in several countries request that the real power injected by wind turbines into the electricity grid should be reduced to maintain the stability of the system. In addition, the WECS should be able to supply the required amount of reactive power to help restore the voltage to its nominal value.

To overcome this, the solution proposed in this work is to adapt the power references during a voltage dip so that during the fault, the stator and rotor currents are maintained at their initial values before the fault.²⁸ The real power is then reduced, and the reactive power is injected into the grid. These power references are given by equations (1) and their detailed derivation is provided in Appendix A.

$$\begin{cases} P_{sref} = \left(\frac{1}{1+g} \right) P_{tmax} \left(\frac{v_F}{v_n} \right) \\ Q_{sref} = Q_{s0} \left[\left(\frac{v_F}{v_n} \right)^2 - \left(\frac{v_F}{v_n} \right) \right] \end{cases} \quad (1)$$

Where g is the DFIG slip, v_F is the voltage at the instant of the fault and v_n is the nominal voltage. When a voltage decrease is detected, the reference powers are re-adjusted to adapt the operation of the machine to the new supply conditions.

However, due to the limited rating of the power converter (around 30% of the rated power), it becomes difficult to achieve full power control for severe fault conditions. The control will be mainly affected by the severity of the fault. So a new control strategy is proposed in this paper to regulate the real and reactive powers of the DFIG via the RSC.

3. Proposed modeling approach for the RSC controller design

Unlike other research studies which consider the flux in the stator constant in amplitude to simplify the control design methodology, the approach proposed in this paper considers the dynamic of the flux during the transients. During a voltage dip, the stator flux will decrease because the stator is directly connected to the network and this should be taken into consideration during the design of the controller.

In a rotating Park reference frame, the direct and quadrature components of the DFIG voltage and flux are expressed as:

$$\begin{cases} v_{sd} = R_s i_{sd} + \frac{d\varphi_{sd}}{dt} - \omega_s \varphi_{sq} \\ v_{sq} = R_s i_{sq} + \frac{d\varphi_{sq}}{dt} + \omega_s \varphi_{sd} \\ v_{rd} = R_r i_{rd} + \frac{d\varphi_{rd}}{dt} - \omega_r \varphi_{rq} \\ v_{rq} = R_r i_{rq} + \frac{d\varphi_{rq}}{dt} + \omega_r \varphi_{rd} \end{cases} \quad (2)$$

$$\begin{cases} \varphi_{sd} = L_s i_{sd} + M i_{rd} \\ \varphi_{sq} = L_s i_{sq} + M i_{rq} \\ \varphi_{rd} = L_r i_{rd} + M i_{sd} \\ \varphi_{rq} = L_r i_{rq} + M i_{sq} \end{cases} \quad (3)$$

The stator real and reactive powers are given by:

$$\begin{cases} P_s = v_{sd} i_{sd} + v_{sq} i_{sq} \\ Q_s = v_{sq} i_{sd} - v_{sd} i_{sq} \end{cases} \quad (4)$$

It should be noted that the quadrature component of the flux is not equal to zero during a voltage dip, hence the stator currents are obtained as:

$$\begin{cases} i_{sd} = \frac{\varphi_{sd} - M i_{rd}}{L_s} \\ i_{sq} = \frac{\varphi_{sq} - M i_{rq}}{L_s} \end{cases} \quad (5)$$

Substituting these currents equations into (3):

$$\begin{cases} \varphi_{rd} = \sigma L_r i_{rd} + \frac{M}{L_s} \varphi_{sd} \\ \varphi_{rq} = \sigma L_r i_{rq} + \frac{M}{L_s} \varphi_{sq} \end{cases} \quad (6)$$

Now, substituting the flux equations into (2) yields:

Control of Wind Energy Systems to Improve LVRT

$$\begin{cases} v_{rd} = R_r i_{rd} + \sigma L_r \frac{di_{rd}}{dt} - \omega_r \sigma L_r i_{rq} - \omega_r \frac{M}{L_s} \varphi_{sq} + \frac{M}{L_s} \frac{d\varphi_{sd}}{dt} \\ v_{rq} = R_r i_{rq} + \sigma L_r \frac{di_{rq}}{dt} + \omega_r \sigma L_r i_{rd} + \omega_r \frac{M}{L_s} \varphi_{sd} + \frac{M}{L_s} \frac{d\varphi_{sq}}{dt} \end{cases} \quad (7)$$

Using equations (4) and (7) the following relationships between the stator powers and the rotor voltages are obtained:

$$\begin{cases} P_s = [v_{rq} - e_d - e_{\varphi q}] \left[\frac{1}{R_r + (\sigma L_r)S} \cdot \left(-\frac{M v_{sq}}{L_s} \right) \right] + \frac{v_{sq} \varphi_{sq}}{L_s} + v_{sd} i_{sd} \\ Q_s = [v_{rd} + e_q + e_{\varphi d}] \left[\frac{1}{R_r + (\sigma L_r)S} \cdot \left(-\frac{M v_{sq}}{L_s} \right) \right] + \frac{v_{sq} \varphi_{sd}}{L_s} - v_{sd} i_{sq} \end{cases} \quad (8)$$

Where e_d and e_q are the coupling terms between axes d and q . $e_{\varphi d}$ and $e_{\varphi q}$ are related to the stator flux and its dynamics. These terms are defined by:

$$\begin{cases} e_d = \omega_r \sigma L_r i_{rd} \\ e_q = \omega_r \sigma L_r i_{rq} \end{cases} \begin{cases} e_{\varphi d} = \frac{M}{L_s} \left(\omega_r \varphi_{sq} - \frac{d\varphi_{sd}}{dt} \right) \\ e_{\varphi q} = \frac{M}{L_s} \left(\omega_r \varphi_{sd} + \frac{d\varphi_{sq}}{dt} \right) \end{cases} \quad (9)$$

To control the powers of the DFIG at the desired references, equations (8) must be reproduced in the opposite direction by imposing rotor voltages on the machine (v_{rq}, v_{rd}). But these equations show that there is a strong coupling between the powers and voltages. Therefore, the control must be designed to compensate for the coupling effect, the variation of rotor speed, the stator flux and the dynamics of the flux. To achieve this, each axis component must be controlled independently i.e. each having its own control loop (power controller and rotor current controllers).

4. Fuzzy Sliding Mode Control

A type of robust control law, simple to calculate and implement, even for nonlinear systems, is sliding mode control. However, once the sliding regime is reached, the discontinuity in the control generates high frequency oscillations, known as chattering. This is a major shortcoming in sliding mode control, as it can lead to imprecise control, and generate noise in the system.³⁰ To eliminate this chattering phenomenon while retaining the robustness and performance, the discontinuous component is replaced by a fuzzy logic structure.³¹

In general, to achieve this type of control two steps must be performed: choice of the sliding surface and the synthesis of the control laws.

4.1. Choice of the sliding surface

Control of Wind Energy Systems to Improve LVRT

The choice of the sliding surface concerns not only the necessary number of these surfaces, but also their shapes depending on the application and the intended purpose. Generally, the number of sliding surfaces is chosen equal to the size of the control system.

To apply this control scheme to the DFIG, four sliding surfaces must be selected to control the real and reactive powers as well as the rotor currents. These surfaces are selected according to the error between the references input signals and the measurement signals.³²

The most commonly used surface to obtain the sliding regime and which guarantees the convergence of the state towards its reference is defined by³³:

$$S(X) = \left(\frac{d}{dt} + \lambda\right)^{n-1} e \quad (10)$$

Where $e = X_{ref} - X$.

If e_1, e_2, e_3 and e_4 denote the errors of the real power, reactive power, quadrature and direct rotor currents respectively, then:

$$\begin{bmatrix} e_1 \\ e_2 \\ e_3 \\ e_4 \end{bmatrix} = \begin{bmatrix} P_{sref} - P_s \\ Q_{sref} - Q_s \\ i_{rqref} - i_{rq} \\ i_{rdref} - i_{rd} \end{bmatrix} \quad (11)$$

Let $n = 1$ in (10), then the control surfaces have the following form:

$$\begin{bmatrix} S(P) \\ S(Q) \\ S(i_{rq}) \\ S(i_{rd}) \end{bmatrix} = \begin{bmatrix} P_{sref} - P_s \\ Q_{sref} - Q_s \\ i_{rqref} - i_{rq} \\ i_{rdref} - i_{rd} \end{bmatrix} \quad (12)$$

4.2. Synthesis of the control laws

The control action is designed to bring the errors e_1, e_2, e_3 and e_4 to zero under any parameter uncertainties and grid disturbances conditions.

Substituting for P_s, Q_s , taking the derivatives of the surfaces and finally substituting the expressions of the currents i_{rq} and i_{rd} from the equations of the voltages v_{rq} and v_{rd} respectively, gives:

$$\begin{bmatrix} \dot{S}(P) \\ \dot{S}(Q) \\ \dot{S}(i_{rq}) \\ \dot{S}(i_{rd}) \end{bmatrix} = \begin{bmatrix} \dot{P}_{s_ref} + \frac{v_{sq}M}{L_s} \left(-\frac{i_{rq}}{\sigma T_r} - \omega_r i_{rd} + \frac{v_{rq}}{\sigma L_r} - \frac{M\omega_r\varphi_{sd} - M\frac{d\varphi_{sq}}{dt}}{L_s L_r \sigma} \right) - A \\ \dot{Q}_{s_ref} + \frac{v_{sq}M}{L_s} \left(-\frac{i_{rd}}{\sigma T_r} + \omega_r i_{rq} + \frac{v_{rd}}{\sigma L_r} + \frac{M\omega_r\varphi_{sq} - M\frac{d\varphi_{sd}}{dt}}{L_s L_r \sigma} \right) + B \\ i_{rq_ref} + \frac{i_{rq}}{\sigma T_r} + \omega_r i_{rd} - \frac{v_{rq}}{\sigma L_r} + \frac{M\omega_r\varphi_{sd} + M\frac{d\varphi_{sq}}{dt}}{L_s L_r \sigma} \\ i_{rd_ref} + \frac{i_{rd}}{\sigma T_r} - \omega_r i_{rq} - \frac{v_{rd}}{\sigma L_r} - \frac{M\omega_r\varphi_{sq} + M\frac{d\varphi_{sd}}{dt}}{L_s L_r \sigma} \end{bmatrix} \quad (13)$$

With $A = (v_{sd}i_{sd} + v_{sq}\varphi_{sq}/L_s)$, $B = (v_{sd}i_{sq} - v_{sq}\varphi_{sd}/L_s)$, $T_r = L_r/R_r$, and i_{rq} , i_{rd} , v_{rq} , v_{rd} are the control vectors, to force the trajectories of the system to converge towards the surfaces.

$$\begin{bmatrix} i_{rq} \\ i_{rd} \\ v_{rq} \\ v_{rd} \end{bmatrix} = \begin{bmatrix} i_{rq}^{eq} + i_{rq}^{fuz} \\ i_{rd}^{eq} + i_{rd}^{fuz} \\ v_{rq}^{eq} + v_{rq}^{fuz} \\ v_{rd}^{eq} + v_{rd}^{fuz} \end{bmatrix} \quad (14)$$

Substituting the above expressions into (13), gives:

$$\begin{bmatrix} \dot{S}(P) \\ \dot{S}(Q) \\ \dot{S}(i_{rq}) \\ \dot{S}(i_{rd}) \end{bmatrix} = \begin{bmatrix} \dot{P}_{s_ref} + \frac{v_{sq}M}{L_s} \left(-\frac{(i_{rq}^{eq} + i_{rq}^{fuz})}{\sigma T_r} - \omega_r i_{rd} + \frac{v_{rq}}{\sigma L_r} - \frac{M\omega_r\varphi_{sd} - M\frac{d\varphi_{sq}}{dt}}{L_s L_r \sigma} \right) - A \\ \dot{Q}_{s_ref} + \frac{v_{sq}M}{L_s} \left(-\frac{(i_{rd}^{eq} + i_{rd}^{fuz})}{\sigma T_r} + \omega_r i_{rq} + \frac{v_{rd}}{\sigma L_r} + \frac{M\omega_r\varphi_{sq} - M\frac{d\varphi_{sd}}{dt}}{L_s L_r \sigma} \right) + B \\ i_{rq_ref} + \frac{i_{rq}}{\sigma T_r} + \omega_r i_{rd} - \frac{(v_{rq}^{eq} + v_{rq}^{fuz})}{\sigma L_r} + \frac{M\omega_r\varphi_{sd} + M\frac{d\varphi_{sq}}{dt}}{L_s L_r \sigma} \\ i_{rd_ref} + \frac{i_{rd}}{\sigma T_r} - \omega_r i_{rq} - \frac{(v_{rd}^{eq} + v_{rd}^{fuz})}{\sigma L_r} - \frac{M\omega_r\varphi_{sq} + M\frac{d\varphi_{sd}}{dt}}{L_s L_r \sigma} \end{bmatrix} \quad (15)$$

During the sliding mode and in steady state, the values of the surface and its derivative, and the fuzzy control are equal to zero. Then equivalent controls quantities are derived from the above equation, and are written as follows:

$$\begin{cases} i_{rq}^{eq} = \frac{\sigma T_r L_s}{v_{sq} M} (\dot{P}_{s_ref} - A) - \sigma T_r \omega_r i_{rd} + \frac{v_{rq}}{R_r} - \frac{M\omega_r\varphi_{sd} - M\frac{d\varphi_{sq}}{dt}}{L_s R_r} \\ i_{rd}^{eq} = \frac{\sigma T_r L_s}{v_{sq} M} (\dot{Q}_{s_ref} + B) + \sigma T_r \omega_r i_{rq} + \frac{v_{rd}}{R_r} + \frac{M\omega_r\varphi_{sq} - M\frac{d\varphi_{sd}}{dt}}{L_s R_r} \end{cases} \quad (16)$$

$$\begin{cases} v_{rq}^{eq} = \sigma L_r \left(\dot{i}_{rqref} + \frac{i_{rq}}{\sigma T_r} + \omega_r i_{rd} \right) + \frac{M \omega_r \varphi_{sd} + M \frac{d\varphi_{sq}}{dt}}{L_s} \\ v_{rd}^{eq} = \sigma L_r \left(\dot{i}_{rdref} + \frac{i_{rd}}{\sigma T_r} - \omega_r i_{rq} \right) - \frac{M \omega_r \varphi_{sq} + M \frac{d\varphi_{sd}}{dt}}{L_s} \end{cases} \quad (17)$$

During the convergence mode, for the condition $S(X)\dot{S}(X) < 0$ to be satisfied, the following must hold:

$$\begin{bmatrix} \dot{S}(P) \\ \dot{S}(Q) \\ \dot{S}(i_{rq}) \\ \dot{S}(i_{rd}) \end{bmatrix} = \begin{bmatrix} -\frac{M v_{sq}}{\sigma T_r L_s} i_{rq}^{fuz} \\ -\frac{M v_{sq}}{\sigma T_r L_s} i_{rd}^{fuz} \\ -\frac{1}{\sigma L_r} v_{rq}^{fuz} \\ -\frac{1}{\sigma L_r} v_{rd}^{fuz} \end{bmatrix} \quad (18)$$

For the input variables (sliding surfaces of the real power P , reactive power Q and rotor currents i_{rd} and i_{rq}) and for the output variables (i_{rq}^{fuz} , i_{rd}^{fuz} , v_{rq}^{fuz} , v_{rd}^{fuz}), the fuzzy sets are defined as: NB (Negative Big), NM (Negative Medium), EZ (Equal Zero), PM (Positive Medium), and PB (Positive Big) and are shown in Figures 2 and 3.

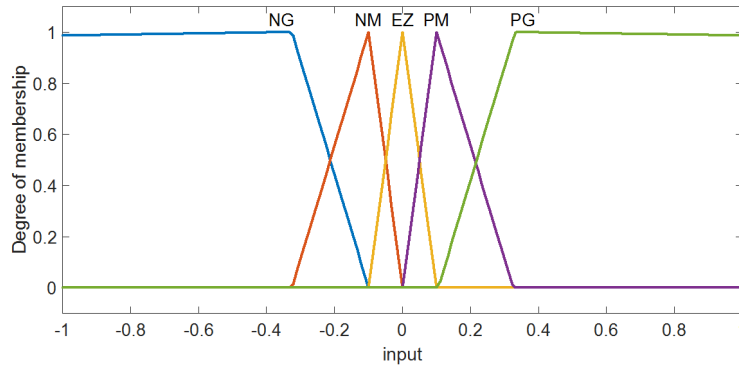


FIGURE 2 Membership functions for the input variables.

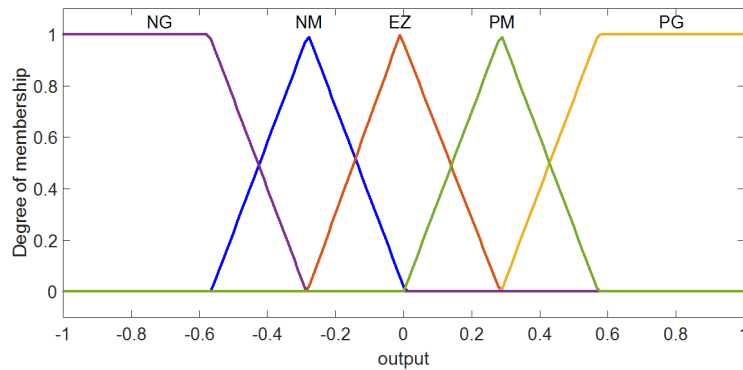


FIGURE 3 Membership functions for the output variables.

The fuzzy rules are given in Table 2. Mamdani’s fuzzy inference and membership function aggregation uses the max operator. The defuzzification of the control output is based on the center of gravity method.

TABLE 2 Fuzzy rule base of the FSMC.

Fuzzy input	NB	NM	EZ	PM	PB
Fuzzy output	NB	NM	EZ	PM	PB

According to the rules presented in Table 2 and the membership functions of Figures 2 and 3, and based on equation (18), it can be noticed that if the surface is positive the fuzzy controller imposes a positive output, hence the derivative of the surface is negative, and therefore the convergence condition is guaranteed. Alternatively, if the surface is negative, the fuzzy controller imposes a negative output, hence the derivative of the surface is positive, and again the convergence condition is achieved.

Figure 4 shows the overall structure of the proposed control scheme.

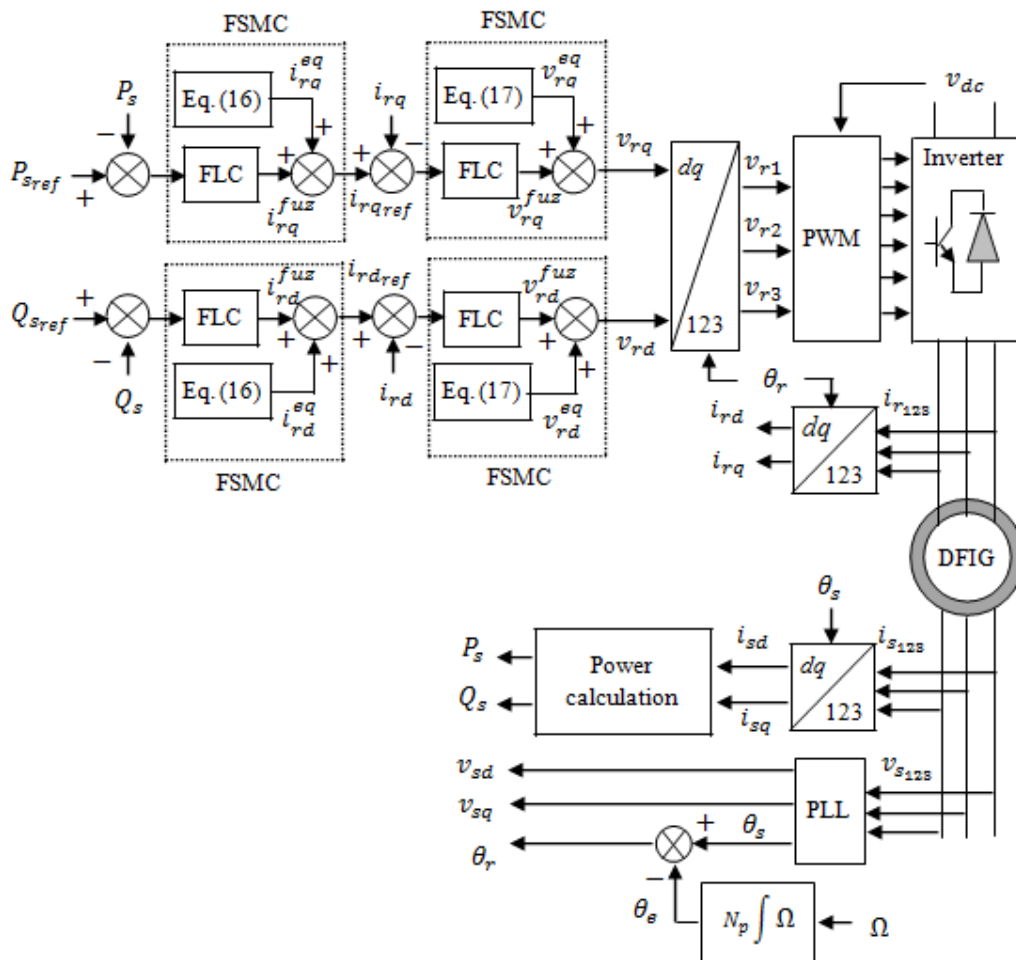


FIGURE 4 Block diagram of the proposed control system.

5. Simulation Results

A simulation study is presented to validate the proposed control approach and demonstrate its robustness and performance during voltage dips. The simulation is based on a 3 MW wind turbine, the parameters of the DFIG and turbine models are listed in Table 3.³⁴ These results are compared with classical vector control.

TABLE 3 DFIG and turbine parameter values.³⁴

P_n	nominal power (MW)	3
U_n	nominal voltage (V)	690
f_n	nominal frequency (Hz)	50
V_{wn}	nominal wind speed (m/s)	13
N_p	pole pairs	2
R_s	stator resistance (m Ω)	2.97
L_s	stator inductance (mH)	12.241
R_r	rotor resistance (m Ω)	3.82
L_r	rotor inductance (mH)	12.1773
M	mutual inductance (mH)	12.12
J	turbine total inertia (kg·m ²)	254
f	turbine total friction coefficient (Nm·s/rad)	0.0024
v_{dcn}	nominal dc-link voltage (V)	1200
C	dc bus capacitor (F)	0.038
R	radius of the blades (m)	45

The simulated LVRT conditions for the wind turbine are as follows:

- The wind turbine must be operating at a critical threshold level before the fault. It should be noted that these are the conditions under which the LVRT requirement is the most difficult to fulfill, because the wind turbine operates at its maximum power and its speed is in the super-synchronous mode.
- Before the fault; the real power injected into the grid is maximum, and the reactive power is zero (unity power factor).
- During the fault, the real power is reduced, and the reactive power is injected into the grid.

The voltage dip considered in this study has been inspired from Danish grid code. It is illustrated in Figure 5 and has the following characteristics:

Control of Wind Energy Systems to Improve LVRT

- Three-phase symmetrical voltages dip (since the term LVRT of national grid codes refer to this type of faults).
- 40% drop in nominal voltage for 0.5 s.
- Linear rise to the nominal voltage over a period of 1 s.

This gradual rise characterizes the inductive loads present on the grid. After fault clearance, these loads will have a high demand of reactive power, which prevent the return of the voltage to its nominal value. This justifies the shape of the voltage dip patterns presented in Figure 5.

Since the duration of the fault is relatively short compared to the fluctuations of the wind speed, the latter will be assumed constant during the fault and equal to $V_w = 13 \text{ m/s}$.

With this wind speed, the wind turbine operates at rated speed, which corresponds to a speed of the DFIG with MPPT control at 1950 rpm, a slip of -30% in super-synchronous mode.

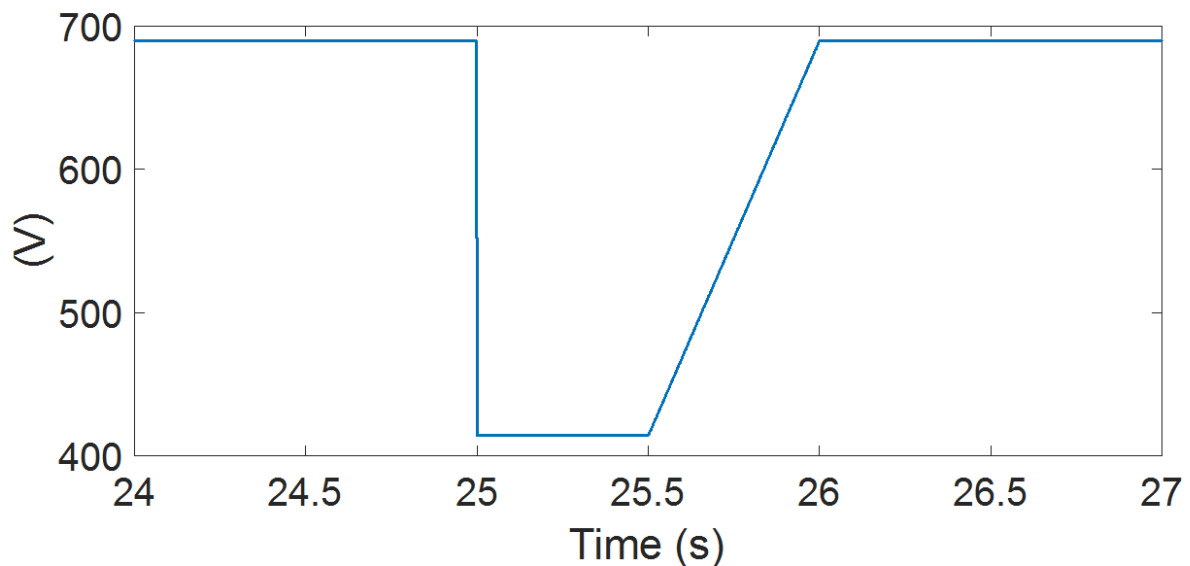


FIGURE 5 Simulated voltage dip under Danish grid code requirements.

Figure 6 compares the responses of the wind turbine system using vector control and the proposed control scheme.

Control of Wind Energy Systems to Improve LVRT

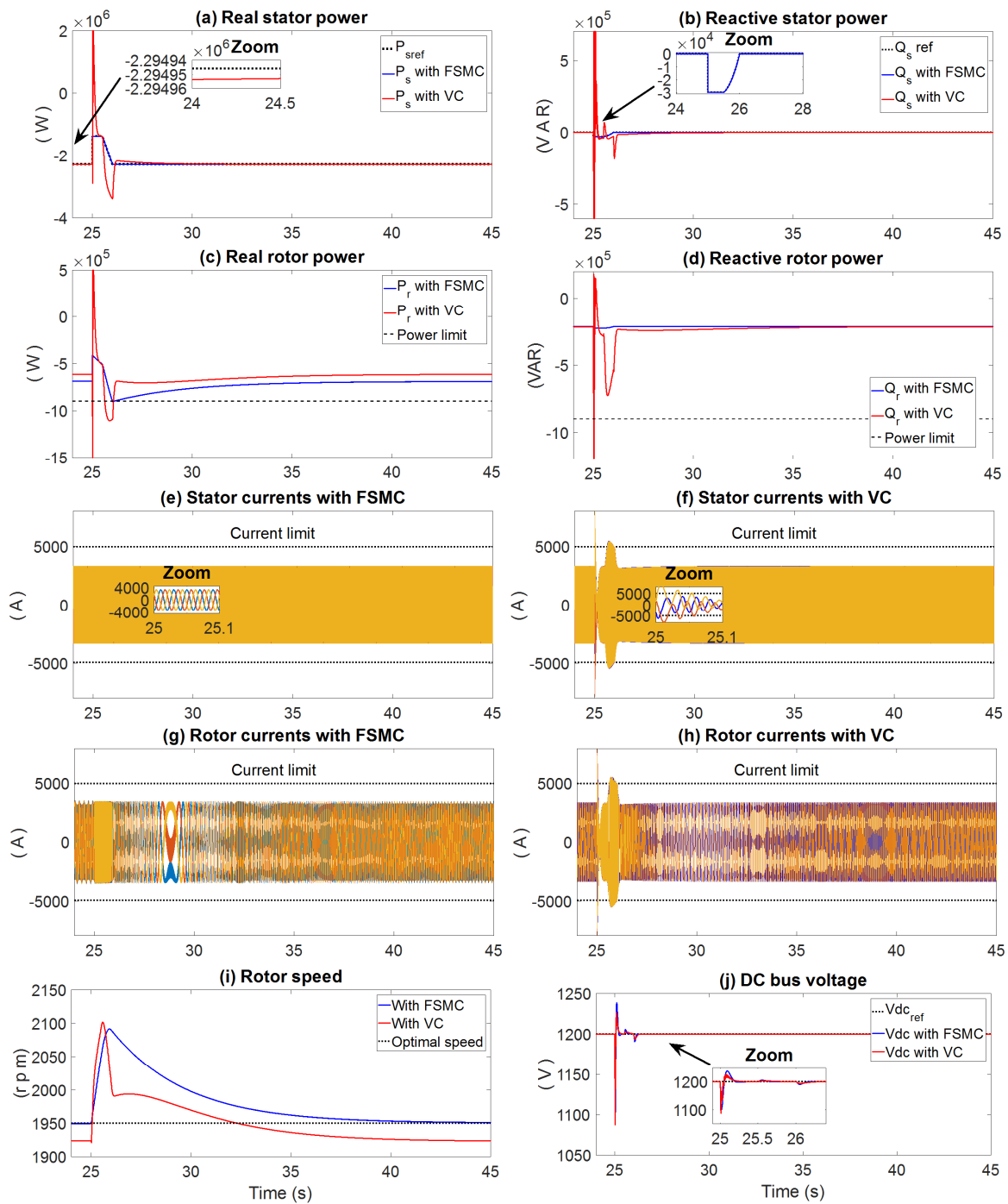


FIGURE 6 Responses of the wind turbine system with FSMC and VC:

- (a) real stator power, (b) reactive stator power, (c) real rotor power, (d) reactive rotor power, (e) stator currents with FSMC, (f) stator currents with VC, (g) rotor currents with FSMC, (h) rotor currents with VC, (i) rotor speed, (j) DC bus voltage.

Figures 6 c-f-h show that when vector control is used during the voltage dip, the stator currents, rotor currents and rotor powers exhibit significant fluctuations above their maximum

Control of Wind Energy Systems to Improve LVRT

acceptable limits (the currents limit is 150% of its rated value, and the rotor powers limit is 30% of its rated value). This will activate the protections so that neither the converter nor the DFIG will be damaged, and it leads to the disconnection of the system. The excursions of the responses of the current and rotor powers are due to the poor tracking of stator powers references (Figures 6 a-b).

On the other hand, when the FSMC is used, the stator powers follow their references perfectly (Figures 6 a-b). The stator and rotor currents are maintained constant as shown in Figures 6 e-g. In addition the rotor powers do not exceed their limits (Figures 6 c-d).

During the fault, the power from the wind is stored as kinetic energy in the rotor (due to its large inertia, the rotor of the wind turbine has a capacity to store energy).²⁵ This causes an increase in the rotor speed (≈ 2100 rpm). Note that this increase is about 40% above the speed of synchronism (1500 rpm) for both control strategies (Figure 6i). For this type of wind turbine the increase in speed is acceptable, since it has a short duration. However if the speed is compared with the speed before fault, an increase of about 9.25% can be observed in the case of VC, and 7.3% in the case of FSMC. This is explained by the fact that with VC the speed is not optimal in the nominal regime, because there is a slight steady-state error in the stator active power as shown in the zoom of Figure 6a.

After fault clearance, the energy stored in the rotor is sent to the grid as active power and subsequently, the rotor speed gradually returns back to its pre-fault value. It can be observed that FSMC leads to a better performance as compared to VC.

The DC bus voltage waveform is shown in Figure 6j. At the onset of the fault, the rotor power demand will be supplied from the DC link, this results in a decrease of the DC bus voltage. When the fault is cleared, this voltage undergoes a disturbance and then is subsequently regulated via the GSC and maintained within an acceptable level.

From these results, it can be noted that with the FSMC there is a good tracking of the reference powers which significantly improve the behavior of the system during dip voltage.

The proposed control design strategy was based on wind turbine model parameters which have been assumed fixed. However, in a real system, such as the wind generator, these parameters are subject to variations due to different physical phenomena such as saturation of inductances, heating of resistors, etc.

Therefore, testing the robustness of the controller under parameter uncertainties is essential. This test is carried out by varying the DFIG model parameters. The resistances are increased by 50%, and the inductances are decreased by 50%. The responses of the real and reactive

stator powers under parameter uncertainties are shown in Figure 7. The results demonstrate a good tracking of the real and reactive powers references when using FSMC.

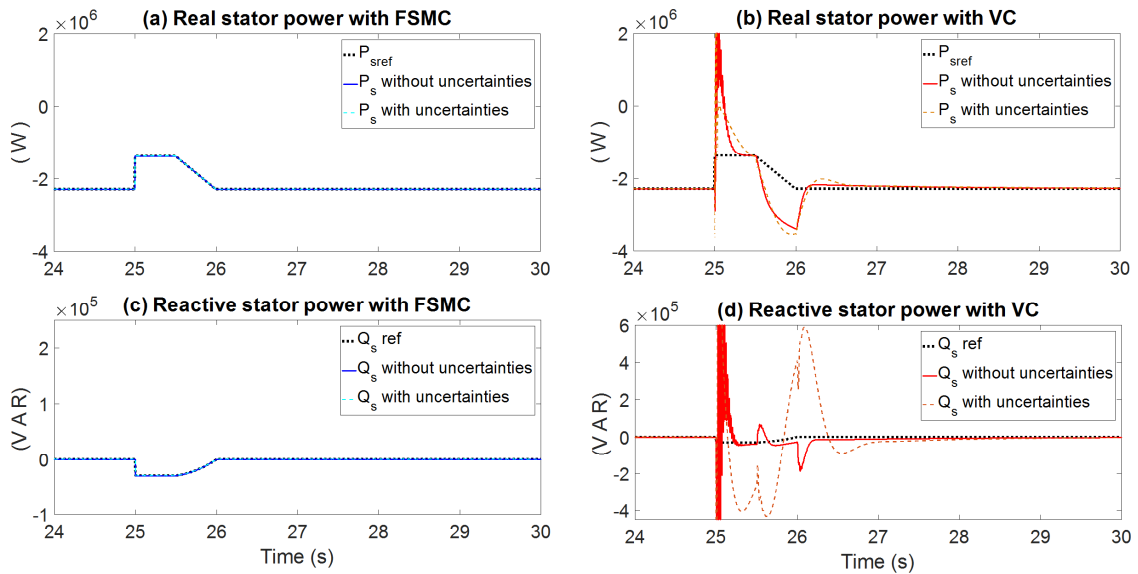


FIGURE 7 Responses of the real and reactive stator powers under parameter uncertainties: (a) real stator power with FSMC, (b) real stator power with VC, (c) reactive stator power with FSMC, (d) reactive stator power with VC

These results show that by adopting the proposed control strategy without additional hardware, the DFIG-based variable-speed wind turbine is able to fulfill the LVRT requirements and remain connected during voltage dips when operating at a critical threshold level (if the voltage dip does not exceed 40% of the nominal voltage).

The strategy for the adaptation of real and reactive powers references during voltage dips ensures that the electrical and mechanical quantities do not exceed their limits. This strategy is very much dependent on the performance of the control scheme of the powers. This has been addressed via the application of FSMC which takes into account the variation of the stator flux.

6. Conclusion

The paper proposed a fuzzy sliding mode control (FSMC) scheme that takes into account the dynamics of the stator flux in the control of real and reactive power of a DFIG-based wind turbine during a voltage dip.

Control of Wind Energy Systems to Improve LVRT

The results demonstrate that FSMC provides a more robust control of the DFIG during the voltage dip conditions as compared to vector control. Indeed, the DFIG was able to successfully overcome the voltage dip without disconnecting from the network. The system was able to quickly regain its initial state of operation.

It should be noted that with FSMC it is possible to improve the capacity of the DFIG to resist against voltage disturbances so as to satisfy the constraints imposed by the LVRT requirements without the need of any auxiliary hardware. However, its capacity is limited by the relatively small size of the power converters.

Appendix A: Calculation of powers references (equation (1))

Under normal conditions, the real and reactive stator powers are expressed as:

$$\begin{cases} P_{sn} = -v_n \frac{M}{L_s} i_{rqn} \\ Q_{sn} = \frac{v_n^2}{\omega_s L_s} - \frac{v_n M}{L_s} i_{rdn} \end{cases} \quad (19)$$

And in the case of fault, these powers are given as:

$$\begin{cases} P_{sF} = -v_F \frac{M}{L_s} i_{rqF} \\ Q_{sF} = \frac{v_F^2}{\omega_s L_s} - \frac{v_F M}{L_s} i_{rdF} \end{cases} \quad (20)$$

To have a power adjustment during the voltage dip, it is necessary that the rotor currents are maintained at the same levels as before fault, i.e. $i_{rqn} = i_{rqF}$ and $i_{rdn} = i_{rdF}$

For this, the following equalities must hold:

$$\begin{cases} P_{sn} \frac{L_s}{M v_n} = P_{sF} \frac{L_s}{M v_F} \\ \frac{L_s}{M v_n} \left(\frac{v_n^2}{\omega_s L_s} - Q_{sn} \right) = \frac{L_s}{M v_n} \left(\frac{v_F^2}{\omega_s L_s} - Q_{sF} \right) \end{cases} \quad (21)$$

Thus the relation between the powers before and during the default is given as follows:

$$\begin{cases} P_{sF} = P_{sn} \left(\frac{v_F}{v_n} \right) \\ Q_{sF} = Q_{sn} \left(\frac{v_F}{v_n} \right) + \frac{v_n^2}{\omega_s L_s} \left[\left(\frac{v_F}{v_n} \right)^2 - \left(\frac{v_F}{v_n} \right) \right] \end{cases} \quad (22)$$

In our study the stator real power is controlled so that the DFIG converts the maximum of the available mechanical power from the turbine such as; if the losses are neglected, the converted real power is expressed by:

$$P_t = P_s + P_r = P_s + g P_s = (1 + g) P_s \quad (23)$$

Control of Wind Energy Systems to Improve LVRT

The stator reactive power is controlled so that the reactive power is zero ($Q_{sn} = 0$).

Therefore, the references of the stator powers are written as equation (1)

$$\begin{cases} P_{sref} = \left(\frac{1}{1+g}\right) P_{tmax} \left(\frac{v_F}{v_n}\right) \\ Q_{sref} = Q_{s0} \left[\left(\frac{v_F}{v_n}\right)^2 - \left(\frac{v_F}{v_n}\right) \right] \end{cases} \quad (24)$$

With $Q_{s0} = v_n^2 / \omega_s L_s$

It should be noted that when the fault is cleared, the ratio $(v_F/v_n) = 1$ and the term $[(v_F/v_n)^2 - (v_F/v_n)] = 0$, hence the reference values of real and reactive power are reset to their values before the fault.

Appendix B: Determination of the PI controllers parameters.

In the control of the RSC, four controllers were used: two for the powers and two for the rotor currents. To simplify the design of the controllers, the RSC is assumed ideal and the coupling terms are neglected. Then, it can be noticed that the transfer functions of the two d and q axes are identical and hence the controllers for the two loops are the same.

The block diagram of the closed-loop q axis control of the RSC is depicted in Figure 8.

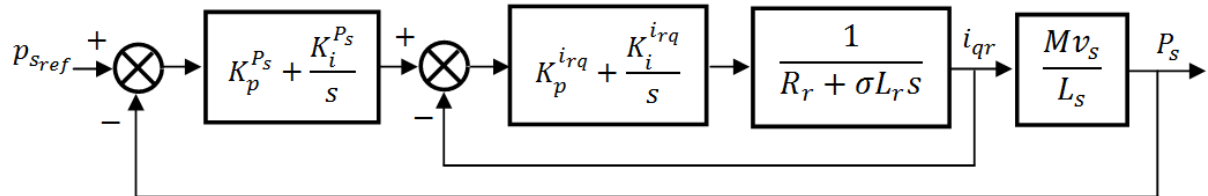


FIGURE 8 Control block diagram in the q axis of the RSC.

Figure 8 shows two control loops: an internal loop for the control of the current and an external loop for the control of the power. For the calculation of the controller parameters of the current loop, a 1st order closed-loop transfer function is used. For the power control loop, a 2nd order closed-loop transfer function is used.

The open-loop transfer function of the current control loop is given by:

$$\left(K_p^{i_{rq}} + \frac{K_i^{i_{rq}}}{s} \right) \frac{1}{R_r + \sigma L_r s} = \frac{1}{T_s} \quad (25)$$

After calculation and identification, the following PI controller parameters are obtained:

Control of Wind Energy Systems to Improve LVRT

$$\begin{cases} K_p^{irq} = \frac{3\sigma L_r}{t_s^{irq}} = 0.0053 \\ K_i^{irq} = \frac{3R_r}{t_s^{irq}} = 0.1146 \end{cases} \quad (26)$$

t_s^{irq} is the settling time of the closed-loop response of the current.

Similarly, for the power control loop, the closed-loop transfer function is given as follows:

$$H_p(s) = \frac{(K_p^{Ps} + K_i^{Ps})Mv_s}{s^2 + \frac{L_s + K_p^{Ps}Mv_s}{TL_s}s + \frac{K_i^{Ps}Mv_s}{TL_s}} \quad (27)$$

The controller parameters are obtained using a simple pole placement. The desired characteristic polynomial is written as follows: $s^2 + 2\gamma s + 2\gamma^2$.

After calculation and identification, the following PI controller parameters are obtained:

$$\begin{cases} K_p^{Ps} = \frac{2\gamma TL_s - L_s}{Mv_s} = 0.006 \\ K_i^{Ps} = \frac{2\gamma^2 TL_s}{Mv_s} = 0.56 \end{cases} \quad (28)$$

References

1. American National Standard (ANSI). IEEE Recommended practices and requirements for harmonic control in electrical power systems. *IEEE Std 519*. 1992.
2. Bollen MHJ. Understanding power quality problems voltage sags and interruptions. New Jersey: John Wiley & Sons; 2000.
3. Mohseni M, Islam SM. Review of international grid codes for wind power integration: diversity, technology and a case for global standard. *Renewable and Sustainable Energy Reviews*. 2012; 16(6):3876-3890.
4. Rolán A, Pedra J, Córcoles F. Detailed study of DFIG-based wind turbines to overcome the most severe grid faults. *Electrical Power and Energy Systems*. 2014; 62:868-878.
5. Gayen PK, Chatterjee D, Goswami SK. An improved low-voltage ride-through performance of DFIG based wind plant using stator dynamic composite fault current limiter. *ISA Transactions*. 2016;62: 333-348.
6. Oriol GB, Adrià JF, Sumper A, Joan B-J. Ride-through control of a doubly fed induction generator under unbalanced voltage sags. *IEEE Transactions On Energy Conversion*. 2008; 23(4):1036-1045.

Control of Wind Energy Systems to Improve LVRT

7. J. J. Justo, F. Mwasilu, and J.-W. Jung. Doubly-fed induction generator based wind turbines: A comprehensive review of fault ride-through strategies. *Renewable and Sustainable Energy Reviews*. 2015; 45: 447-467.
8. I. Ngamroo and T. Karaipoom. Cooperative Control of SFCL and SMES for Enhancing Fault Ride Through Capability and Smoothing Power Fluctuation of DFIG Wind Farm. *IEEE Transactions on Applied Superconductivity*. 2014; 24(5):1-4.
9. K. Ibrahima and C. Zhao. Modeling of wind energy conversion system using doubly fed induction generator equipped batteries energy storage system. *4th International Conference on Electric Utility Deregulation and Restructuring and Power Technologies (DRPT)*, 2011; 1780-1787.
10. S. I. Gkavanoudis and C. S. Demoulias. A combined fault ride-through and power smoothing control method for full-converter wind turbines employing Supercapacitor Energy Storage System. *Electric Power Systems Research*. 2014; 106: 62-72
11. G. Pannell, D. J. Atkinson, and B. Zahawi. Minimum-Threshold Crowbar for a Fault-Ride-Through Grid-Code-Compliant DFIG Wind Turbine. *IEEE Transactions on Energy Conversion*. 2010; 25(3):750-759.
12. M. Molinas, J. A. Suul, and T. Undeland. Low Voltage Ride Through of Wind Farms With Cage Generators: STATCOM Versus SVC. *IEEE Transactions on Power Electronics*. 2008; 23(3): 1104-1117.
13. C. Wessels, F. Gebhardt, and F. W. Fuchs. Fault Ride-Through of a DFIG Wind Turbine Using a Dynamic Voltage Restorer During Symmetrical and Asymmetrical Grid Faults. *IEEE Transactions on Power Electronics*. 2011; 26(3): 807-815.
14. Xiang D, Ran L, Tavner PJ, Yang S. Control of a doubly fed induction generator in a wind turbine during grid fault ride-through. *IEEE Transactions On Energy Conversion*. 2006;21:652-662.
15. Seman S, Niiranen J, Arkkio A. Ride-through analysis of doubly fed induction wind-power generator under unsymmetrical network disturbance. *IEEE Transactions On Power Systems*. 2006;21:1782-1789.
16. Nian H, Song Y, Zhou P, He Y. Improved direct power control of a wind turbine driven doubly fed induction generator during. *IEEE Transactions On Energy Conversion*. 2011;26:976-986.
17. Song Z, Shi T, Xia C, Chen W. A novel adaptive control scheme for dynamic performance improvement of DFIG-Based wind turbines. *Energy*. 2012;38:104-117.

Control of Wind Energy Systems to Improve LVRT

18. Phan VT, Lee HH. Improved predictive current control for unbalanced stand-alone doubly-fed induction generator-based wind power systems. *IET Electric Power Applications*. 2011;5:275-287.
19. Peng L, Colas F, Francois B, Li Y. A modified vector control strategy for DFIG based wind turbines to ride-through voltage dips. *13th European Conference on Power Electronics and Applications*, 2009.
20. Anaya-lara O, Hughes FM, Jenkins N, Strbac G. Rotor flux magnitude and angle control strategy for doubly fed induction generators. *Wind Energy*. 2006;9:479-495.
21. Xiao-ming Li, Xiu-yu Zhang, Zhong-wei Lin, Yu-guang Niu. An Improved Flux Magnitude and Angle Control With LVRT Capability for DFIGs. *IEEE Transactions on Power Systems*. 2018
22. Saad NH, Sattar AA, Mansour AEM. Low voltage ride through of doubly-fed induction generator connected to the grid using sliding mode control strategy. *Renewable Energy*. 2015;80:583-594.
23. Benbouzid M, Beltran B, Amirat Y, Yao G, Han J, Mangel H. Second-order sliding mode control for DFIG-based wind turbines fault ride-through capability enhancement. *ISA Transactions*. 2014;53:827-833.
24. Raju SK, Pillai GN. Design and real time implementation of type-2 fuzzy vector control for DFIG based wind generators. *Renewable Energy*. 2016;88:40-50.
25. Theodoros DV, Xanthi IK, Nicholas AV. A genetic algorithm-based low voltage ride-through control strategy for grid connected doubly fed induction wind generators. *IEEE Transactions On Power Systems*. 2014; 29(3):1325-1334.
26. Mohammad JM, Afef F. A new fault ride-through control for DFIG-based wind energy systems. *Electric Power Systems Research*. 2017; 146: 258-269.
27. Vandai L, Xinran L, Yong L, Tran LTD, Caoquyen L. An innovative control strategy to improve the fault ride-through capability of DFIGs based on wind energy conversion systems. *Energies*. 2016; 69(9):1-23.
28. Kammoun S, Sallem S, Kammoun MBA. Backstepping control for low-voltage ride through enhancement of DFIG-based wind turbines. *Arabian Journal for Science and Engineering*. 2017; 42(12):5083-5099.
29. M. Ezzat, M. Benbouzid, S. M. Muyeen, and L. Harnefors, "Low-voltage ride-through techniques for DFIG-based wind turbines: state-of-the-art review and future trends," in *IECON 2013 - 39th Annual Conference of the IEEE Industrial Electronics Society*. 2013; 7681–7686.

Control of Wind Energy Systems to Improve LVRT

30. Furat M, Eker İ. Second-order integral sliding-mode control with experimental application. *ISA Transactions*. 2014;53:1661-1669.
31. Ardjoun SAEM, Abid M. Fuzzy sliding mode control applied to a doubly fed induction generator for wind turbines. *Turkish Journal of Electrical Engineering & Computer Sciences*.2015;23(6): 1673-1686
32. Utkin VI. Sliding mode control design principles and applications to electric drives. *IEEE Transactions On Industrial Electronics*. 1993;40:23–36.
33. SLOTINE J-JE, LI W. Applied Nonlinear Control. Englewood Cliffs New Jersey: Prentice Hall; 1991.
34. Lohde R, Jensen S, Knop A, Fuchs FW. Analysis of three phase grid failure and Doubly Fed Induction Generator ride-through using crowbars. *Proceedings of the 12th European Conference on Power Electronics and Applications (EPE 2007)*, Aalborg, Denmark, September 2007.